NUMERICAL ANALYSIS OF TRANSPORT PHENOMENA IN SEMINCONDUCTING DEVICES AND STRUCTURES. 2. INVESTIGATION OF CHARGE CARRIER MOTION IN AN I^2L ELEMENT

I. I. Abramov and V. V. Kharitonov

UDC 621.382.82.001:530.1

The results of a numerical experiment, using two-step vector relaxation, on transport of mobile charge carriers in an integrated circuit element with injection are presented.

There are currently only a few papers [1, 2] concerning the two-dimensional numerical analysis of transport of charge carriers in a single-collector I^2L elements, which form the basis for large integrated circuits with injection feeding [3]. This is explained by the complexities that arise in solving the system of nonlinear partial differential transport equations [4], which in its turn greatly complicates the design and development of such circuits.

The difficulties of such an analysis are related to the fundamental two-dimensional nature of the processes occuring in these structures, which are a result of the internal interaction of two types of transistors with vertical (n–p–n) and horizontal (p–n–p) structures with common collector–base and base–emitter regions. This essentially involves mutual compensation and unbalance of charge-carrier flows in the most diverse directions.

In this paper, we demonstrate the efficiency of the techniques developed in [4] for the example of a numerical analysis of charge transport processes in the single-collector I^2L element with a submerged n^+ layer shown in Fig. 1 (the geometric dimensions of the structure analyzed are given in μm).

The analysis was performed for two operational states of the inverter based on such an element [1], arising when 1) a rectilinear bias voltage is applied to the resistive contact of the injector, while the bias in the remaining contacts equals zero and 2) rectilinear bias voltages are applied to the injector and base contacts, i.e., the horizontal p–n–p transistor is saturated.

The fundamental system of equations (see (1)-(5) in [4]) was solved assuming that the Boltzmann statistics are valid as in [1, 2]. In so doing, the effect of the high level of doping, whose main effect is to narrow the width of the forbidden band [5], was not included in the analysis for the following reasons:

a) its magnitude is uncertain [6, 7], and it is difficult to ascertain which of the theoretical formulations is correct from the experimental results [8];

b) the experimental results on narrowing of the forbidden band also include other effects (deionization of the impurity, degeneracy, etc.) [9] and therefore they depend on the specific structure of the device on which the measurements were performed;

c) the mechanism of two-step recombination–generation (following the Shockley–Reed–Hall model [2, 8]) has a dominant effect on the results of modeling.

But, since the effect of the high level of doping is manifested only with impurity concentrations in the active regions of the device exceeding 20^{23}-10^{24} $1/m^3$ [10, 11], the results presented in this paper were obtained for low levels of these concentrations.

The surface concentrations for different regions of the device are presented in Table 1.

The distribution of donors N_d and acceptors N_a in the I^2L element analyzed was approximated, according to [3], by exponentials. The structure consists of a common epitaxial p substrate with impurity concentration $N_a = 0.3\ 10^{22}\ 1/m^3$.

Belorussian Institute of Railroad Transportation Engineers, Gomel. V. I. Lenin Belorussian State University, Minsk. Translated from Inzhenerno-Fizicheskii Zhurnal, Vol. 44, No. 3, pp. 474-480, March, 1983. Original article submitted November 23, 1981.

 0022-0841/83/4403-0334$07.50

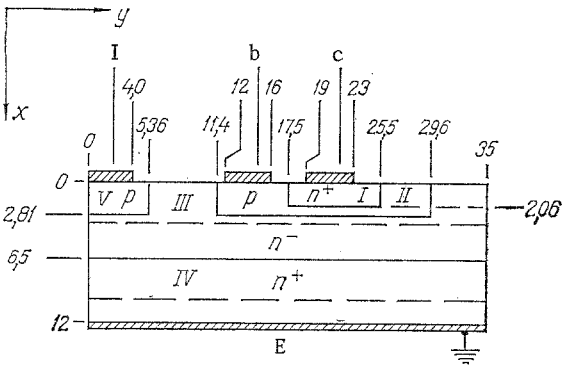

Fig. 1. View of the I^2L structure analyzed.

TABLE 1. Concentration of Donors N_d and Acceptors N_a in the Device

Region in Fig. 1	I	II	III	IV	V
Surface conc. (m^{-3})	$N_d = 0{,}5 \cdot 10^{26}$	$N_a = 0{,}5 \cdot 10^{25}$	$N_d = 0{,}8 \cdot 10^{22}$	$N_d = 0{,}5 \cdot 10^{25}$	$N_a = 0{,}5 \cdot 10^{25}$

The numerical experiments were performed using a program for two-dimensional numerical analysis of I^2L elements "PNAIIL" [12] (for Boltzmann statistics), written in the FORTRAN IV language for the ES computer using the technique proposed in the first part of this work [4]. We should point out here that the development of the program for solving this problem, which is still largely an art and requires from 1 to 5 man years [13] and more for one type of device only, can be greatly accelerated using the procedure described in the first part of this work.

The PNAIIL program is based on the following:

1) Sharfetter–Hummel formulation of the continuity equation;

2) a method for choosing the initial approximation [14] modified as indicated in the first part of this work [4];

3) a universal method, the Hummel and Siedman–Chu methods, from [15] and the two-step VRS method from part 1 of this work;

4) Chebyshev's cyclical method [16] and the Buleev–Stone method [17, 18] (for continuity equations only) for solving the system of linear algebraic equations.

All quantities were determined at nodes by a quasiuniform, over the regions of the device, grid of spatial discretization. The total number of basic unknowns in the approximate algebraic problem was $5 \cdot 10^3$ and higher.

Figure 2a shows the behavior of $|\delta\Psi|_{\max_i}$ (curve 1 shows the number of Newton iterations) for the Siedman–Chu method (S–C) (curve 1) single-step [15] (curve 2) and two-step VRS (curve 3), methods in which, to increase the rate of convergence as well as to decrease the machine time used, two iterations of sections 2 and 3 of the method in [4] are performed. Thus a single iteration of the two-step method requires no greater computational time than two iterations of the Siedman–Chu method. In the present numerical experimental the voltages of the resistive contacts have the following values: $V_i = 0.7$ V; $V_e = V_b = V_c = 0$ V. It is evident from the graphs that the rate of convergence of the two-stepped VRS method (TS) is much higher than that of S–C method and higher than that of the single-step method (SS) proposed in [15]. Comparing the amounts of machine time used, we note that for the SS method ≈ 20 equivalent S–C iterations are required, while for the TS method approximately 18 iterations are required (i.e., the TS method is approximately 1.1 times more efficient than the SS method).

A numerical experiment taking into account the effect of Auger recombination, using the generalized two-step VRS method, was performed for the same bias voltages. The maximum deviation was approximately 0.7% for the collector current. This indicates the negligibly small effect of this recombination mechanism for the device examined and for the bias voltages given, agreeing with the results in [8], which were obtained for a bipolar transistor.

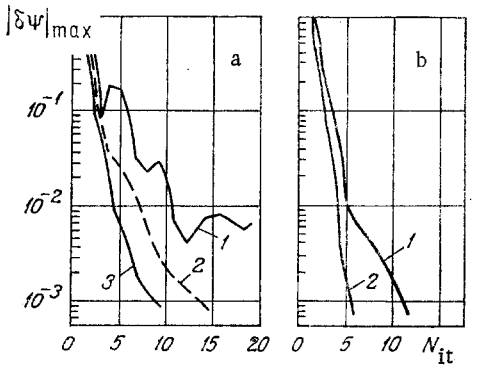

Fig. 2. Investigation of the convergence of different methods ($\delta\Psi$ in normalized units kTq = 0.0258 V): *a* — $\tau_n = \tau_p = 50$ nsec; 1) Siedman—Chu method; 2) method in [15]; 3) two-step VRS method; b) $\tau_n = \tau_p = 1$ nsec; 1) method in [15]; 2) two-step VRS method.

We note the advantage of the TS method compared to the SS method in calculating the currents in the device. Thus, for bias voltages $V_i = 0.7$ V, $V_b = 0.67$ V, $V_c = 0.01$ V, $V_e = 0$ V (saturated horizontal p—n—p transistor), approximately the same values of the currents were obtained with 7 (14 equivalent) and 15 (20 equivalent) iterations of the TS method. The lifetime of carriers varied from $\tau_n = \tau_p = 50$ nsec to $\tau_n = \tau_p = 1$ nsec.

The efficiency of the two-step methods examined in the first part of this work, which have a higher rate of convergence, increases with increasing level of recombination.

Figure 2b shows the behavior of $|\delta\Psi|_{max_i}$ using the SS method (curve 1) and the TS method (curve 2) for much shorter carrier life times. In this case, $V_i = 0.7$ V, $V_e = V_b = V_c = 0$ V, and the computational time used was as follows: 16 and 12 equivalent S—C iterations for SS and TS, respectively. Therefore, in this numerical experiment, the proposed two-step VRS method turned out to be more efficient than the single-step VRS method approximately by a factor of 1.3.

From the physical point of view, the study of the behavior of n and p concentrations, the potential Ψ, and the current densities inside the I^2L element are of greatest interest. The dominating effects for this structure are modulation of the conductivity, current reflection are current leakage.

These effects are essentially analogs of the reflection of the emitter current [19, 20], modulation of the base conductivity [21], and transverse leakage of the collector current [22, 23], encountered in planar bipolar transistors with vertical structure [24].

Figures 3a-c show the results of the investigations performed on the effect of the decrease of carrier lifetimes on the total current density $[j_x^{0,7}]$ as a function of the coordinate y for the bias voltages $V_i = 0.7$ V, $V_b = V_c = V_e = 0$ V in two sections, which are shaded in Fig. 1. For given biases, high injection levels (i.e., $p > N_d - N_a$) are observed in regions next to the injector.

Comparison of Figs. 3a and b (the continuous lines correspond to currents along the x axis, and the dashed lines correspond to the reverse currents) shows that for these lifetimes the results do not differ qualitatively. However, we note that for $\tau_n = \tau_p = 500$ nsec, compared to the case when $\tau_n = \tau_p = 50$ nsec, we have the following:

1) more efficient reflection of injector current from the emitter, manifested in the much lower value of the emitter current (i.e., higher β of the horizontal p—n—p transistor);

2) lower value of the injector current density, which agrees with the classical theory of rectilinearly biased p—n junctions [25];

3) increase in the peak of the reflected injector current and current flowing into the base (dashed line).

As the carrier lifetime decreases to $\tau_n = \tau_p = 1$ nsec, the efficiency of emitter reflection drops to zero and, therefore, the efficiency of the horizontal p—n—p transistor decreases (Fig. 3c). We also note the pronounced hump in the total current density curve, which in this case lies between the injector and base regions. The reason for this phenomenon appar-

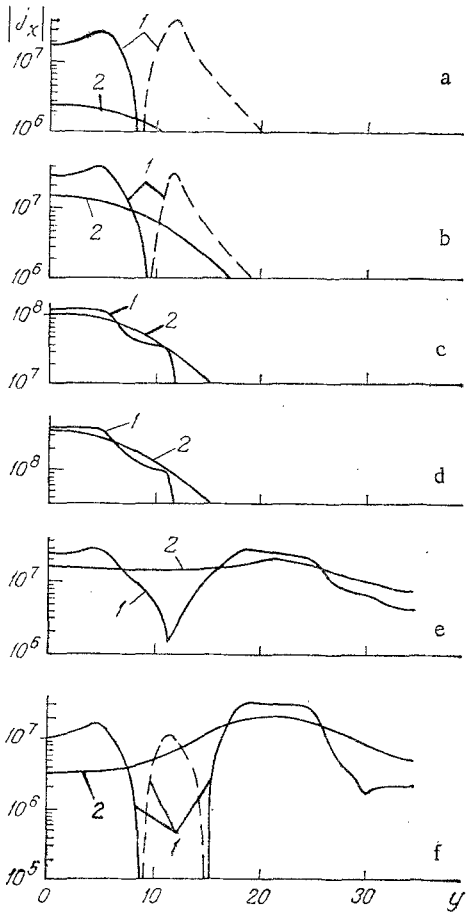

Fig. 3. Current density distributions (j_x in normalized units $7.25 \cdot 10^{-3}$ A/m^2): a) $\tau_n = \tau_p = 500$ nsec: 1) section at x = 3.4 μm; 2) 9.6 μm; b) $\tau_n = \tau_p = 50$ nsec: 1) section at x = 3.4 μm; 2) 9.6 μm; c) $\tau_n = \tau_p = 1$ nsec, $V_i = 0.7$ V: 1) section at x = 3.4 μm; 2) 9.6 μm; d) $\tau_n = \tau_p = 1$ nsec, $V_i = 0.8$ V: 1) section at x = 3.4 μm; 2) 9.6 μm; e) $\tau_n = \tau_p = 50$ nsec: 1) section at x = 3.4 μm; 2) 9.6 μm; f) $\tau_n = \tau_p = 500$ nsec: 1) section at x = 3.4 μm; 2) 9.6 μm.

ently lies in the stronger vertical injection of the accumulated charge (compared to $\tau_n = \tau_p = 50$ nsec) in the n^- region between the injector and base and the absence, in this case, of a countermoving compensated flow with corresponding magnitude.

The change in the injector current as a whole is due to the decrease in the number of accumulated mobile charge carriers in the bulk of the n^- region under the injector, as well as unbalance of the drift and diffusion current components which mutually compensate at zero bias voltages:

a) smaller diffusion components with increasing τ:

b) increase in the role of drift current components with decreasing τ:

c) overall increase (absolute and relative) of role of the majority charge-carrier current with decreasing carrier lifetime τ.

The change in the reflected injector current into the base at the edge of this region is determined primarily by the increase in the number of accumulated mobile charge carriers, caused by leakage of injector current into the bulk of the n^- emitter region, as well as by the decrease in the diffusion current components with decreasing τ and increase in the drift components with increasing τ.

The results presented confirm the importance of studying two-dimensional effects in I^2L cells.

Figure 3d shows the total current density $|j_x^{0.8}|$ for the following bias voltages: V_i = 0.8 V, $V_e = V_c = V_b = 0$ V.

Comparison of these results with the results presented in Fig. 3c permits writing an approximate expression for the total current densities for these values of τ as

$$\ln j_x^{0.8}(y) \approx \ln j_x^{0.7}(y) + C; \quad (1)$$

in addition, the quantity C is practically independent of x and, therefore, approximately equals the logarithm of the ratio of the emitter currents. We note that expression (1) represents a relation between the total current densities, which is analogous to the Moll–Ross relations for electronic emitter current densities in n–p–n transistors, well-known from the classical one-dimensional theory of a planar bipolar transistor [24], but for values of the m factor differing considerably from unity. The latter circumstance is a result of the fact that no assumptions were made concerning the negligible value of the recombination–regeneration, which is assumed in deriving the Moll–Ross relation [24].

Figure 3e and f presents the results for a more complicated case: V_i = 0.7 V, V_b = 0.67 V, V_e = 0 V, V_c = 0.01 V, when the horizontal p–n–p transistor is saturated. The concentration of the emitter junction current [3], beginning in this case in the n^- region, is evident (this is especially clear in Fig. 3f). This manifestation of the effect is related to the considerable modulation of conductivity in this region at such bias voltages. The complexity of the analysis in this case is determined by the fact that the collector–base and emitter–base junctions are rectilinearly biased and, in addition, the bias of the latter is higher than that of the former. The increase in the current concentration with increasing carrier lifetime, which agrees with [3], is also evident. An interesting fact is observed here: the practically complete absence of emitter current leakage for carrier lifetimes $\tau_n = \tau_p$ = 50 nsec (Fig. 3e). This is related, therefore, to two basic mechanisms: 1) decrease in injector current reflection from the emitter and 2) concentration of the emitter current.

It should be noted that the theoretical investigations performed on the effect of the decrease of the lifetime on the behavior of the I^2L element could also be useful for a deeper study of the action of radiation on the structures, since in this case the carrier lifetime is observed to decrease [26].

NOTATION

$\delta\Psi$, perturbation of the electrostatic potential Ψ, relative to which the linearized Poisson equation is formulated; τ_n, τ_p, charge carriers (electrons and holes); V_i, V_e, V_b, V_c, voltages on the resistive contacts of the injector, emitter, base, and collector, respectively; $j_x^{0.7}$, $j_x^{0.8}$, components of the total current densities, oriented along the x axis with injector voltages of 0.7 and 0.8 V, respectively; β, gain in current of the horizontal p–n–p transistor in a scheme with a common injector; N_{it}, number of iterations of the method.

LITERATURE CITED

1. W. L. Engl and H. Dirks, "Numerical device simulation guided by physical approaches," Proc. NASE/CODE 1 Conf., Dublin, June 27-29, 1979; B. T. Browne and J. J. H. Miller, (ed.), Boole Press, Dublin, Vol. 12 (1979), pp. 65-93.
2. T. Toyabe, K. Ujiie, T. Okabe, M. Nagata, and M. S. Mock, "Method and application of a two-dimensional analysis of I^2L," Trans. Inst. Electron Commun. Eng. Jpn., J 62-C, No. 3, 215-222 (1979).
3. N. A. Avaev, V. N. Dulin, and Yu. E. Naumov, Large Integrated Circuits with Injection Feeding [in Russian], Sovet-skoe Radio, Moscow (1977).
4. I. I. Abramov and V. V. Kharitonov, "Numerical analysis of transport phenomena in semiconducting devices and structures. 1. General principles for constructing methods for solving the fundamental system of equations," Inzh.-Fiz. Zh., 44, No. 2, 284-293 (1983).
5. V. I. Fiztul', Strongly Doped Semiconductors [in Russian], Nauka, Moscow (1967).
6. R. Van Overstraeten, H. De Man, and R. Mertens, "Transport equations in heavily doped silicon," IEEE Trans., ED-20, No. 3, 290-298 (1973).
7. M. S. Mock, "Transport equations in heavily doped silicon and the current gain of a bipolar transistor," Solid-State Electron., 16, 1251-1259 (1973).
8. M. S. Adler, "Achieving accuracy in transistor and thyristor modeling," Int. Electron. Devices Meet., Washington, D.C., Dec. 4-6, 1978, New York, pp. 550-555.

9. M. S. Adler, "A method for achieving and choosing variable density grids in finite-difference formulations and the importance of degeneracy and band gap narrowing in device modeling," Proc. NASE-CODE 1 Conf., Dublin, June 27-29, 1979; B. T. Browne and J. J. H. Miller (ed.), Dublin: Boole Press, Vol. 12 (1979), pp. 3-30.
10. M. S. Mock, "On heavy doping effects and the injection efficiency of silicon transistors," Solid-State Electron., 17, No. 8, 819-824 (1974).
11. J. W. Slotboom and H. C. De Graaf, "Bandgap narrowing in silicon bipolar transistors," IEEE Trans., ED-24, No. 8, 1123-1125 (1977).
12. I. I. Abramov, "Algorithms for numerical analysis of bipolar semiconducting devices and their comparison," Abstracts of Reports at the Scientific-Technical Conference "Problems of Using Current Radiophysical Methods for Increasing the Efficiency of Performing and Automating Scientific Investigations," Minsk, May 21-22, 1981, Pt. 2, p. 54.
13. M. Reiser, "Computing methods in semiconductor problems," Lect. Notes Comput. Sci., 10, 441-446 (1974).
14. S. G. Mulyarchik and I. I. Abramov, "Choice of initial approximation in the numerical analysis of bipolar semiconducting devices," Izv. Vyssh. Uchebn. Zaved., Radiofiz., 24, No. 6, 59-67 (1981).
15. I. I. Abramov and S. G. Mulyarchik, "Method of vector relaxation of systems in problems of multidimensional analysis of semiconducting devices," Izv. Vyssh. Uchebn. Zaved., Radioelektron., 24, No. 6, 59-67 (1981).
16. D. E. Potter, Computational Physics, Wiley (1973).
17. N. I. Buleev, "Numerical method for solving two- and three-dimensional diffusion equations," Mat. Sb., Nov. Ser., 51 (93), No. 2, 227-238 (1960).
18. H. L. Stone, "Iterative solution of implicit approximations of multidimensional partial differential equations," SIAM J. Numer. Anal., 5, Sept. 530-558 (1968).
19. N. H. Fletcher, "Some aspects of the design of power transistors," Proc. IRE, 43, No. 5, 551-559 (1955).
20. J. R. Hauser, "The effects of distributed base potential on emitter-current injection density and effective base resistance for stripe transistor geometries," IEEE Trans., ED-11, No. 5, 238-242 (1964).
21. W. M. Webster, "On the variation of junction-transistor current-amplification factor with emitter current," Proc. IRE, 42, No. 6, 914-920 (1954).
22. A. Van der Ziel and D. Agouridis, "The cutoff frequency falloff in UHE transistors at high currents," Proc. IEEE (Lett.), 54, No. 3, 411-412 (1966).
23. R. J. Whittier and D. A. Tremer, "Current gain and cutoff frequency falloff at high currents," IEEE Trans., ED-16, No. 1, 39-57 (1969).
24. Ya. A. Fedotov (ed.), Planar Silicon Transistor [in Russian], Sovet-skoe Radio, Moscow (1973).
25. I. P. Stepanenko, Foundations of Microelectronics [in Russian], Sovet-skoe Radio, Moscow (1980).
26. V. S. Vavilov, Action of Radiation on Semiconductors [in Russian], Fizmatgiz, Moscow (1963).